Reactive Path Planning for Micro Air Vehicles using Bearing-only Measurements

Rajnikant Sharma* Jeffery B. Saunders† Randal W. Beard‡

MAGICC LAB, Brigham Young University, Provo, Utah, 84602, USA

Abstract

Autonomous path planning of Micro Air Vehicles(MAVs) in an urban environment is a challenging task because urban environments are dynamic and have variety of obstacles, and the locations of these obstacles may not be available a priori. In this paper we develop a reactive guidance strategy for collision avoidance using bearing-only measurements. The guidance strategy can be used to avoid collision from circular obstacles and to follow straight and curved walls at safe distance. The guidance law moves a obstacle in the sensor field-of-view to a desired constant bearing angle, which causes the MAV to maintain a constant distance from the obstacle. We use sliding mode control theory to derive the guidance law, which is fast, computationally inexpensive, and guarantees collision avoidance.

1 Introduction

Recently, the use micro air vehicles (MAVs) in several civil and military applications have increased significantly. Smaller MAVs have different applications that require them to operate in urban terrains. Urban environments

*Graduate research assistant, Department of Electrical and Computer Engineering, Brigham Young University, Student Member AIAA.

†Systems Engineer at Raytheon Missle Systems, Tucson, AZ.

‡Professor, Department of Electrical and Computer Engineering, Brigham Young University, Senior Member AIAA.

consist of trees, poles, buildings, walls, tunnels, canyons, etc. Since the urban environments are dynamic in nature, locations of some objects may not be known a priori, it is necessary to develop local path planning algorithms, which are fast enough to avoid pop up obstacles and guarantee obstacle avoidance.

In this paper, we consider two types of object for collision avoidance including cylindrical obstacles and walls. Almost all the obstacles in an urban terrain can be modelled as cylindrical obstacles or walls. Our focus is to develop reactive guidance strategies for collision avoidance, which uses bearing-only measurements. There exists a suite of different sensors, which can provide bearing measurements. One of such sensors is camera, which fits in with size and weight requirements of a small MAV, and has high information to weight ratio.

Obstacle avoidance and path planning algorithms have been extensively studied in literature, especially for ground robots. For example, Probability Road Map (PRM) methods generate random points in the configuration space and connect the points to create a navigation map of the environment [1, 2, 3]. Another probabilistic planning technique is the Rapidly-Expanding Random Tree (RRT) [4, 5], which is often used in conjunction with fixed-wing air vehicles. RRTs generate random points in the configuration space and connect them to a tree of other points such that the non-holonomic constraints of the vehicle are satisfied. Points unable to connect to the tree are removed. While these methods and their many variants (e.g. [6, 7, 8, 9, 1, 10, 11]) have shown considerable success, they often require significant computation time to generate paths around obstacles. Therefore, in environments where pop-up threats are common, a reactive planner with fixed computational cost may be more appropriate. Reactive obstacle avoidance methods have been developed in previous work using dynamic replanning [12], potential fields [13], simulated annealing [14], and predefined maneuvers [15].

Potential fields is a common reactive obstacle avoidance technique[15, 16, 13], but unfortunately it, and many of its variants, only guarantee a high probability of avoiding obstacles. Since collisions in flight can be catastrophic, aircraft require guaranteed obstacle avoidance. In previous work, we develop a reactive method that generates a path to one side of an obstacle field, which is used in conjunction with waypoint paths [17]. While the method in [17] produced paths around obstacles, it was susceptible to oscillations in the presence of multiple obstacles. In order guarantee collision

avoidance, we need a deterministic guidance strategy that reacts to obstacles within the sensor field-of-view and requires limited computational resources. A deterministic collision avoidance guidance strategy for stationery cylindrical objects is proposed in [18]. However, the guidance strategy in [18] requires both range from obstacle and bearing to obstacle to compute the control law. In this paper, we extend the work done in [18] by re-deriving the guidance strategy using sliding mode control such that it does not require range from the obstacle, and uses only bearing to obstacle to avoid obstacles. Furthermore, we also extend the guidance strategy to avoid collision from straight and curved walls.

The basic concept of collision avoidance guidance strategy is to move the obstacle in the sensor plane and maintain the obstacle at a desired constant bearing angle. By keeping the obstacle at a desired bearing angle in the sensor plane causes the MAV to converge at a constant distance from the obstacle and guarantees collision avoidance. The reactive guidance strategy is fast, computationally inexpensive, and guarantee collision avoidance, which keeps the obstacle in the field-of-view and minimizes the chances of collision.

The paper is organized as follows. In Section 2 we formulate detail the relative equations of motion and formulate the collision avoidance problem. In Section 3 we derive bearing-only guidance laws for collision avoidance from cylindrical obstacle and following a wall. We provide simulation results in Section 4 and provide our conclusions in Section 5.

2 Model and Problem Formulation

In this paper, we consider a fixed wing MAV with a strapdown camera mounted parallel to the x-axis of the body frame and is equipped with an onboard autopilot with inner loop control of roll, pitch, airspeed, and altitude. A forward looking camera allows objects to be viewed in the short reachable region of the MAV. Equation of motion of a MAV flying at constant altitude can be written as

$$\begin{pmatrix} \dot{x} \\ \dot{y} \\ \dot{\psi} \end{pmatrix} = \begin{pmatrix} V\cos\psi \\ V\sin\psi \\ \frac{g}{V}\tan\phi \end{pmatrix} \tag{1}$$

where $[x, y]^\top$ is the position vector, ψ is the heading, V is the airspeed, ϕ is the commanded roll angle, g is the gravity constant, and we have assumed

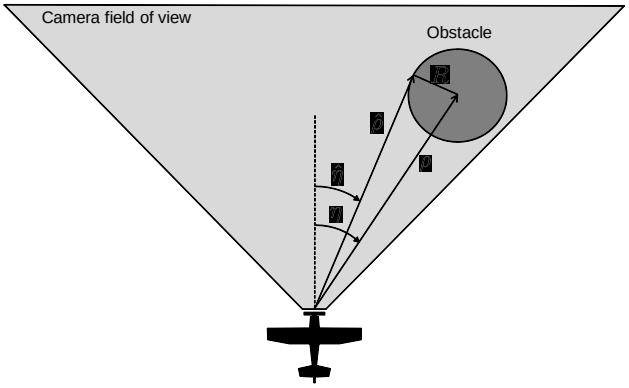

Figure 1: A conceptual view of the MAV approaching an obstacle. The guidance law moves the obstacle to the edge of the camera field-of- view to avoid collision.

zero ambient wind.

Almost all the obstacles in urban environments can be modelled either as a cylindrical obstacle (e.g, trees, poles, small buildings, etc.) or a wall (large, buildings, tunnels, subways, canyons, etc). In next two subsections we discuss relative motions of equation for cylindrical obstacles and walls, which will be used to derive the guidance strategies.

2.1 Relative equation of motion between cylindrical obstacle and the MAV

The geometry of the cylindrical obstacle avoidance problem is shown in Figure 1 where ρ is the range from the MAV to the center of the obstacle and η is the bearing to the center of the obstacle. The relative equations of motion for the system are

$$\dot{\rho} = -V \cos \eta, \tag{2}$$

$$\dot{\eta} = \frac{V}{\rho} \sin \eta - \frac{g}{V} \tan \phi. \tag{3}$$

We will assume that the obstacle is a cylinder of radius R, and pose the guidance problem with respect to the range and bearing to the edge of the

cylinder as shown in Figure 1 and from Figure 1 we have that

$$R = \rho \sin(\eta - \hat{\eta}) \tag{4}$$

$$\hat{\rho} = \rho \cos(\eta - \hat{\eta}). \tag{5}$$

Differentiating (4) and (5) with respect to time and using Equations (2) and (3) we get the modified relative equations of motion

$$\dot{\hat{\eta}} = -\frac{g}{V} \tan \phi + \frac{V}{\hat{\rho}} \sin \hat{\eta}, \tag{6}$$

$$\dot{\hat{\rho}} = -V \left[\cos \hat{\eta} - \frac{R}{\hat{\rho}} \sin \hat{\eta} \right]. \tag{7}$$

2.2 Relative equation of motion between wall and the MAV

The geometry between the MAV and a wall is shown in Figure 2. This geometry is similar to geometry for stationery obstacle, however in this case, the obstacle is moving on the wall. We consider a virtual cylindrical obstacle of radius R. This obstacle moves on the wall with velocity

$$V_w = V \cos(\psi - \psi_w) \tag{8}$$

where $\psi - \psi_w$ is the relative orientation of wall with respect to MAV heading, V_w is the projection of MAV velocity on the wall. The relative orientation of the wall $\psi - \psi_w$ is directly computed from the image plane using the the image segmentation followed by orientation computation of the segment. By keeping the virtual obstacle at desired bearing angle, the portion of the wall always stays in the image plane and MAV can fly along the wall and maintain a safe distance from the wall. The minimum distance between wall and MAV is given as

$$R_{min} = \rho \sin(\psi - \psi_w + \hat{\eta}) \tag{9}$$

To avoid collision from the wall the MAV should maintain $R_{min} > 0$ for all time. From Figure 2 the equations of relative motion between MAV and the obstacle moving on wall can be written as

$$\dot{\rho} = V_w \cos(\psi - \psi_w - \eta) - V \cos(\eta), \tag{10}$$

$$\dot{\eta} = -\frac{V_w \sin(\psi - \psi + w + \eta) - V \sin(\eta)}{\rho} + \frac{g}{V} \tan(\phi). \tag{11}$$

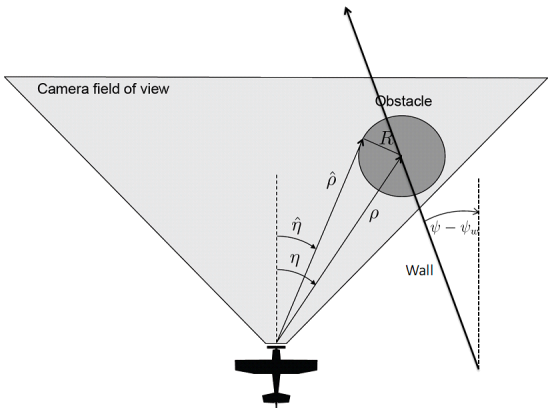

Figure 2: A conceptual view of the MAV approaching a wall. The guidance law keeps the wall at the edge of the camera field of view to avoid collision.

Differentiating (4) and (5) with respect to time and using Equations (10) and (11) we get the modified relative equations of motion

$$\dot{\hat{\eta}} = \frac{V \sin \hat{\eta}}{\hat{\rho}} - \frac{V_w \sin(\psi_w - \psi + \hat{\eta})}{\hat{\rho}} + \frac{g}{V} \tan \phi, \tag{12}$$

$$\dot{\hat{\rho}} = \frac{R}{\hat{\rho}} V \sin \hat{\eta} + V_w \cos(\psi_w - \psi + \hat{\eta}) - \frac{R}{\hat{\rho}} V_w \sin(\psi_w - \psi + \hat{\eta}) - V \cos \hat{\eta}. \tag{13}$$

3 Bearing-only guidance strategies

Our approach is to push the edge of the obstacle to a specified angle η_d in the image plane. By keeping obstacle at a desired bearing angle the MAV maintains safe distance from the obstacle. Also, keeping the obstacle in the field-of-view is important because if the obstacle is pushed out of the field of view of the camera, then it can no longer be tracked by the guidance algorithm and a collision may occur. Following two subsections detail the collision avoidance guidance strategies for a cylindrical obstacle and a wall.

3.1 Guidance strategy for Cylindrical obstacle

In this subsection we derive the control law for cylindrical obstacle. If $\bar{\eta}$ is the field of view of the camera, then we desire that $|\eta| \leq \bar{\eta}$. Let $|\eta_d| < \bar{\eta}$ be

the desired position of the edge of the obstacle in the image plane. We use Lyapunov's stability theory to move the obstacle at a desired bearing angle in the image plane.

3.1.1 Control law for cylindrical obstacle using range and bearing measurement

For comparison purpose, we re-derive the control law [18] for cylindrical obstacle.

Consider the Lyapunov function candidate

$$W = \frac{1}{2}(\hat{\eta} - \eta_d)^2.$$

Differentiating with respect to time gives

$$\dot{W} = (\hat{\eta} - \eta_d)\left(-\frac{g}{V}\tan\phi + \frac{V}{\hat{\rho}}\sin\hat{\eta}\right).$$

Therefore, selecting the guidance law as

$$\phi = \tan^{-1}\left(\frac{V^2}{g\hat{\rho}}\sin\hat{\eta} + \frac{Vk}{g}(\hat{\eta} - \eta_d)\right), \tag{14}$$

gives

$$\dot{W}_1 = -k(\hat{\eta} - \eta_d)^2,$$

which implies that $\hat{\eta}(t) \to \eta_d$. The control law (14) is a function of both range and bearing measurement.

3.1.2 Control law for cylindrical obstacle using bearing-only measurement

To make control law in (14) independent of range from the obstacle we use sliding mode control to derive the control law. Suppose we can design a control law that constraints the motion of the system to the manifold $s = \hat{\eta} - \hat{\eta_d} = 0$, where $\hat{\eta} = \hat{\eta_d}$. The motion on this manifold is independent of $\frac{V\sin\hat{\eta}}{\hat{\rho}}$. The objective is to bring the states to this manifold. Consider Lyapunov function candidate $V = \frac{1}{2}s^2$. Differentiate V to obtain

$$\dot{V} = s\left(\frac{V\sin\hat{\eta}}{\hat{\rho}} - \frac{g}{V}\tan\phi\right) \tag{15}$$

$$\leq |s|\frac{V|\sin\hat{\eta}|}{\hat{\rho}_{min}} - s\frac{g}{V}\tan\phi \tag{16}$$

where $\hat{\rho}_{min} > 0$ is the lower bound on $\hat{\rho}$. Choosing

$$\phi = \tan^{-1} \frac{V}{g} \left\{ \left(\frac{|V \sin \hat{\eta}|}{\hat{\rho}_{min}} + \beta_0 \right) sat(\frac{\hat{\eta} - \hat{\eta}_d}{\epsilon}) \right\} \tag{17}$$

where $\beta_0 > 0$ yields

$$\dot{V} \leq -\beta_0 |\hat{\eta} - \hat{\eta}_d| < 0, \ \forall \ |\hat{\eta} - \hat{\eta}_d| > \epsilon \tag{18}$$

Therefore, when $|\hat{\eta} - \hat{\eta}_d| > \epsilon$, $|s(t)|$ is strictly decreasing, until it reaches the set $\{|s| \leq \epsilon\}$ in finite time and remains inside thereafter and $|\hat{\eta} - \hat{\eta}_d| \leq \epsilon$.

By holding the edge of a cylindrical object at angle η_d in the camera field of view the MAV will orbit the object, on a circular trajectory of radius $R\sqrt{1 + \tan^2 \eta_d}$ [18], as shown in Figure 3. If the MAV is following a waypoint path and an obstacle appears in the image, the collision avoidance strategy is then to push the edge of the obstacle to an angle of η_d in the image plane using guidance strategy (14), until the MAV moves past the obstacle and can resume tracking its original path.

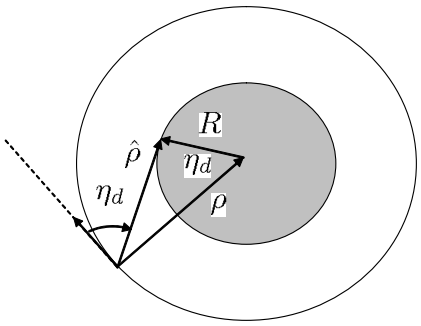

Figure 3: By keeping the object at angle η_d in the camera field of view, the MAV converges to an orbit of radius $R\sqrt{1 + \tan^2 \eta_d}$ [18].

3.2 Guidance strategy for following a wall

If $\bar{\eta}$ is the field of view of the camera, then we desire that $|\eta| \leq \bar{\eta}$. Let $|\eta_d| < \bar{\eta}$ be the desired position of the edge of the virtual obstacle on the wall in the image plane.

3.2.1 Control law for following a wall using range and bearing measurement

To derive the control law for wall following, we choose a Layapunov candidate function as

$$W = \frac{1}{2}(\hat{\eta} - \eta_d)^2$$

and differentiate to obtain

$$\dot{W} = (\hat{\eta} - \eta_d)(\frac{V \sin\hat{\eta}}{\hat{\rho}} + \frac{V_w \sin(\psi - \psi_w + \hat{\eta})}{\hat{\rho}} + \frac{g}{V}\tan\phi)$$

Therefore, picking the guidance law

$$\phi = \tan^{-1}(-\frac{V^2}{\hat{\rho}g}\sin\hat{\eta} + \frac{1}{\hat{\rho}g}VV_w \sin(\psi_w - \psi + \hat{\eta}) - \frac{Vk}{g}(\hat{\eta} - \eta_d)) \tag{19}$$

gives

$$\dot{W} = -k(\hat{\eta} - \eta_d)^2$$

which implies that $\eta_1(t) \to \eta_d$.

3.2.2 Control law for following a wall using bearing-only measurement

To make control law in (19) independent of range from the obstacle we use sliding mode control to derive the control law. We choose the sliding manifold $s = \hat{\eta} - \hat{\eta_d}$ and consider Lyapunov function candidate $V = \frac{1}{2}s^2$. Differentiate V to obtain

$$\dot{V} = s\left(\frac{V\sin\hat{\eta} - V_w \sin(\psi - \psi_w + \hat{\eta})}{\hat{\rho}} - \frac{g}{V}\tan\phi\right) \tag{20}$$

$$\leq |s|\frac{V|\sin\hat{\eta}| + |V_w||\sin(\psi - \psi_w + \hat{\eta})|}{\hat{\rho}_{min}} - s\frac{g}{V}\tan\phi \tag{21}$$

Choosing

$$\phi = \tan^{-1}\frac{V}{g}\left\{\left(\frac{|V\sin\hat{\eta}| + |V_w||\sin(\psi - \psi_w + \hat{\eta})|}{\hat{\rho}_{min}} + \beta_0\right) sat(\frac{\hat{\eta} - \hat{\eta}_d}{\epsilon})\right\} \tag{22}$$

yields

$$\dot{V} \leq -\beta_0 |\hat{\eta} - \hat{\eta}_d| < 0, \ \forall \ |\hat{\eta} - \hat{\eta}_d| > \epsilon \tag{23}$$

Therefore, when $|\hat{\eta} - \hat{\eta}_d| > \epsilon$, $|s(t)|$ is strictly decreasing, until it reaches the set $\{|s| \leq \epsilon\}$ in finite time and remains inside thereafter and $|\hat{\eta} - \hat{\eta}_d| \leq \epsilon$.

Remark 3.1 *It should be noted that if we replace $V_w = 0$ in controller for wall in* (19) *and (22) we get controller equation for a stationary obstacle in (14) and (18) respectively. Therefore, only one controller in (22) can be used for collision avoidance from both cylindrical obstacles and walls.*

Guidance law in (19) enables the MAV to maintain the virtual obstacle at a constant bearing angle in the image plane. This indirectly helps the MAV to maintain safe distance from wall while following the wall.

4 Simulation Results

In this section we include simulation results to validate the collision avoidance algorithm. Some of the simulation parameters are; $V = 15m/s$,$k = 0.5$, $\beta_0 = 0.5$, and $\hat{\rho}_{min} = 1$.

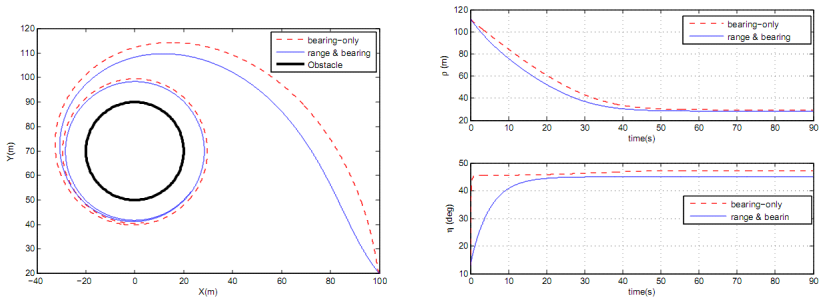

(a) MAV trajectory around a cylindrical obstacle of radius 20m

(b) Range and bearing plots

Figure 4: Cylindrical obstacle avoidance

We start with a stationary cylindrical obstacle of radius $R = 20m$. Figure 4(a) shows the trajectory of MAV around the obstacle using normal controller and sliding mode controller respectively. For both controllers, the MAV converges to a circular trajectory around obstacle of radius $R\sqrt{1 + \tan^2 \eta_d}$.

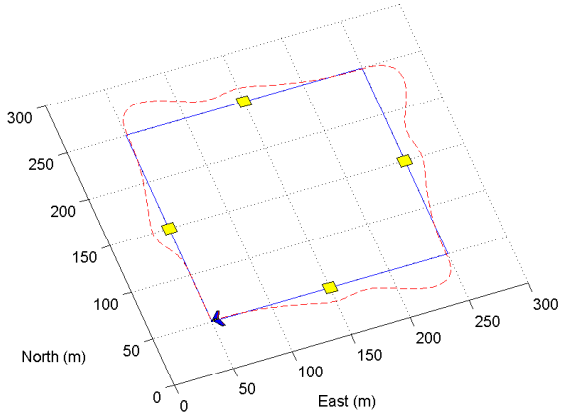

Figure 5: The results of a simulation are shown. The dashed line shows the path of the MAV in tracking the waypoint path and avoiding obstacles. The MAV successfully avoids the obstacles.

In Figure 4(b) it can be seen that the states using sliding mode control are almost equivalent to the states using normal controller. Figure 5 shows the flight path of the MAV with multiple cylindrical obstacles in the initial flight path. It can be seen that MAV avoids all the obstacles successfully using the sliding mode controller.

Trajectories of MAV, close to a straight wall with orientation $\psi_w = 60^o$, using both normal and sliding mode controllers are shown in Figure 6(a). For both controllers the MAV converges on same trajectory parallel to the wall. Figure 6(b) shows that the $\psi \to \psi_w$, $\hat{\eta} \to \hat{\eta}_d$, and $R_{min} \to R_f > R \sin \hat{\eta}_d$. The guidance strategy can also follow and avoid collision from a curved wall. Figure 7(a) shows the trajectory of a MAV along a sinusoidal wall. It can be seen that the MAV also moves along a sinusoidal trajectory while maintains safe distance from the wall. The Figure 7(b) shows the plots of ψ, $\hat{\eta}$, ρ, and R_{min}, which are generated using both normal and sliding mode controller. It can be seen that $R_{min} > R \sin(\hat{\eta}_d)$, hence, collision is avoided successfully.

5 Summary and Conclusions

In this paper, we develop vision based collision avoidance algorithms to avoid collision from different types of popup obstacles. The algorithm moves a ob-

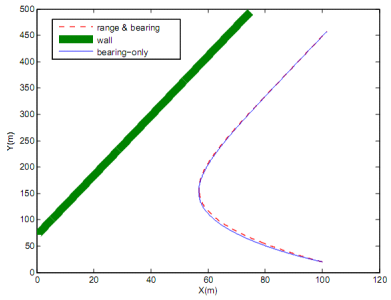

(a) MAV trajectory along a straight wall with orientation $\psi_w = 60^o$

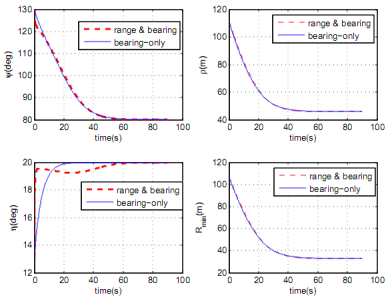

(b) MAV heading, bearing, range, and R_{min} plots

Figure 6: Straight wall following

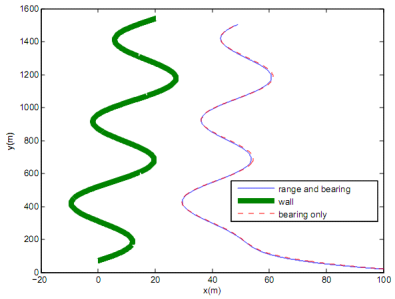

(a) MAV trajectory along a sinusoidal wall

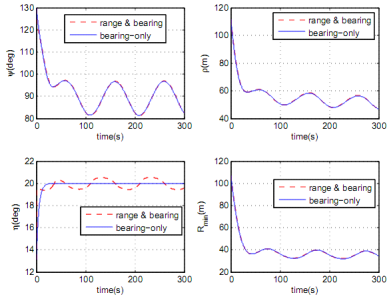

(b) MAV heading, bearing, range, and R_{min} plots

Figure 7: Sinusoidal wall following

stacle in the image plane to a desired constant bearing angle. By keeping the obstacle at a constant bearing angle causes the MAV to maintain a constant distance from the obstacle. Since a camera only provides bearing measurement to obstacles, we modify the algorithm using sliding mode control such that that depth measurement is not required for the computation of the control input. The collision avoidance algorithms are fast, computationally inexpensive, and guarantee collision avoidance.

Acknowledgement

This work was partially supported by the Air Force Research Laboratory, Munitions Directorate under SBIR contract No. FA 8651-07-C-0094 to Scientific Systems Company, Inc. and Brigham Young University, and by AFOSR contract No. FA 9550-07-1-0167.

References

[1] Saha, M. and Latombe, J.-C., "Finding narrow passages with probabilistic roadmaps: the small step retraction method," International Conference on Intelligent Robots and Systems, August 2005, pp. 622–627.

[2] Amato, N. M. and Wu, Y., "A Randomized Roadmap Method for Path and Manipulation Planning," *Proceedings of the IEEE International Conference on Robotics and Automation*, Minneapolis, MN, 1996, pp. 113–120.

[3] Kavraki, L. E., Švestka, P., Latombe, J., and Overmars, M., "Probabilistic Roadmaps for Path Planning in High-Dimensional Configuration Spaces," *IEEE Transactions on Robotics and Automation*, Vol. 12, No. 4, 1996, pp. 566–580.

[4] Cheng, P., Shen, Z., and LaValle, S. M., "Using Randomization to Find and Optimize Trajectories for Nonlinear Systems," *Proceedings of Annual Allerton Conference on Communications, Control, Computing*, 2000.

[5] Kim, J. and Ostrowski, J. P., "Motion Planning of Aerial Robot using Rapidly-exploring Random Trees with Dynamic Constraints," *Proceedings of the IEEE International Conference on Robotics and Automation*, Taipei, Taiwan, September 2003, pp. 2200–2205.

[6] Kuffner, J. J. and LaValle, S. M., "RRT-Connect: An Efficient Approach to Single-Query Path Planning," *Proceedings of the IEEE International Conference on Robotics and Automation*, San Francisco, CA, April 2000, pp. 995–1001.

[7] LaValle, S. M., "Rapidly-Exploring Random Trees: A New Tool for Path Planning," TR 98-11, Computer Science Dept., Iowa State University.

[8] LaValle, S. M. and Kuffner, J. J., "Rapidly-Exploring Random Trees: Progress and Prospects," *Algorithmic and Computational Robotics: New Directions*, edited by B. R. Donald, K. M. Lynch, and D. Rus, A. K. Peters, Wellesley, MA, 2001, pp. 293–308.

[9] LaValle, S. M. and Kuffner, J. J., "Randomized Kinodynamic Planning," Vol. 20, No. 5, May 2001, pp. 378–400.

[10] Sun, Z., Hsu, D., Jiang, T., Kurniawati, H., and Reif, J. H., "Narrow Passage Sampling for Probabilistic Roadmap Planning," *IEEE Transactions on Robotics*, Vol. 21, No. 6, December 2005, pp. 1105–1115.

[11] Kuffner, J.J., J. and LaValle, S., "RRT-connect: An efficient approach to single-query path planning," *IEEE International Conference on Robotics and Automation*, Vol. 2, 2000, pp. 995–1001.

[12] Schwarzer, F., Saha, M., and Latombe, J.-C., "Adaptive Dynamic Collision Checking for Single and Multiple Articulated Robots in Complex Environments," *IEEE Transaction On Robotics*, Vol. 21, No. 3, June 2005, pp. 338–353.

[13] Vadakkepat, P., Tan, K. C., and Ming-Liang, W., "Evolutionary artificial potential fields and their application in real time robot path planning," *Proceedings of the 2000 Congress on Evolutionary Computation*, Vol. 1, July 2000, pp. 256–263.

[14] Park, M. G., Jeon, J. H., and Lee, M. C., "Obstacle avoidance for mobile robots using artificial potential field approach with simulated annealing," *IEEE International Symposium on Industrial Electronics*, Vol. 3, June 2001, pp. 1530–1535.

[15] Ghosh, R. and Tomlin, C., "Maneuver Design for Multiple Aircraft Conflict Resolution," *Proceedings of the American Control Conference*, June 2000.

[16] Barraquand, J., Langlois, B., and Latombe, J. C., "Numerical potential field techniques for robot path planning," *IEEE Transaction On Systems, Man, and Cybernetics*, Vol. 22, No. 2, March/April 1992, pp. 224–241.

[17] Saunders, J. B., Call, B., Curtis, A., Beard, R. W., and McLain, T. W., "Static and Dynamic Obstacle Avoidance in Miniature Air Vehicles," *AIAA Infotech@Aerospace*, September 2005.

[18] Saunders, J. and Beard, R., "Reactive Vision Based Obstacle Avoidance Camera Field of View Constraints," *Guidance Navigation and Control Confrence*, 2008.